Geochemistry versus grain-size relations of sediments in the light of comminution, chemical alteration, and contrasting source rocks

H. VON EYNATTEN[1] and R. TOLOSANA-DELGADO[2]

[1] Abt. Sedimentologie/Umweltgeologie, Geowissenschaftliches Zentrum, Universität Göttingen Göttingen, Germany, hilmar.von.eynatten@geo.uni-goettingen.de

[2] Dept. d'Enginyeria Hidràulica, Marítima i Ambiental, Laboratori d'Enginyeria Marítima (LIM/UPC) Universitat Politècnica de Catalunya, Barcelona, Spain

Abstract

Around 170 sediment samples from glacial and proximal glacio-fluvial deposits have been analysed for their geochemical composition. Samples derive from two strongly contrasting source areas (granitoids vs. amphibolite) and cover a broad grain-size range from coarse sand to clay. Following descriptive data evaluation, the relation of sediment geochemical composition versus grain size is modelled using linear regression techniques in the Aitchison geometry of the simplex in order to (i) describe the effects of comminution on the composition of individual grain size fractions, (ii) describe the influence of inherited mineral-specific grain-size distributions for contrasting source rocks, and (iii) to test for any potential influence of chemical weathering.

Results indicate strong overall grain-size control on sediment composition that is largely reflecting the greater grain-size control on mineralogy. Comminution leads to overall strong enrichment of sheet silicates in the fine-grained fraction at the expense of quartz and, less pronounced, feldspars. Specific elements such as Ca, P, and Ti related to certain minerals do not follow this general trend and clearly indicate source-rock dependent enrichment of certain minerals (e.g. apatite, Ti-minerals) in medium grain-size fractions. Estimates of mineral compositions obtained from a geometric endmember approach support these conclusions. Chemical weathering is shown to be negligible.

1. Introduction

Geochemical compositions of sediments and sedimentary rocks depend on (i) grain size, and (ii) various sediment forming processes such as erosion of contrasting parent rocks, comminution, chemical weathering in situ and on transit, and hydraulic sorting during transport and final deposition (e.g. Weltje and von Eynatten 2004). To quantify these relations we aim at building empirical-statistical models based on field data in which one or two of the above mentioned processes are dominant, so that the effect of the process can be studied in isolation, i.e. without further modifications or feedbacks by other processes. Here we will largely focus on the relation between mechanical comminution and grain size involving inherited grain-size distribution from parent rocks. Future steps may involve other processes such as chemical weathering and hydraulic sorting in order to build a comprehensive model of sediment generation that works in different geological settings and environmental conditions.

At CoDaWork'08 we presented a "log-linear model of grain-size (GS) influence on the geochemistry of sediments" based on a single data set of glacial sediment derived from a single largely homogenous source-rock unit (von Eynatten and Tolosana-Delgado, 2008). Samples covered a broad grain size range from very coarse sand ($-1 < \phi < 0$) to clay ($\phi > 9$), where $\phi = -\log_2(d)$, being d the average diameter of the grain. Results for the limited case study suggested that relations between chemical composition and grain-size are largely controlled by comminution due

Egozcue, J.J., Tolosana-Delgado, R. and Ortego, M.I. (eds.)
ISBN: 978-84-87867-76-7

to glacial friction, whereas chemical weathering plays a negligible role. Moreover, clear steps in the linear regression model at around the sand-silt transition (ϕ=4) and at fine silt grade (ϕ=8) were interpreted to document inherited GS characteristics of the source rocks.

This data set has now been extended towards contrasting source rocks under similar geologic conditions, i.e. mafic amphibolite source rocks have been added to the felsic granitoid rocks existing in the first data set. All samples were investigated for the chemical composition of major and selected trace elements for in total 11 GS fractions to cover the entire GS spectrum that is usually relevant for siliciclastic sediments.

For the statistical evaluation of the data set we use compositional biplot analysis (Aitchison 1990), compositional linear trends including testing for step functions (von Eynatten and Tolosana-Delgado 2008, Tolosana-Delgado and von Eynatten 2010), and a stoichiometric inversion endmember algorithm developed for calculating mineral composition from geochemical data (Tolosana-Delgado et. al, in press). The latter is extremely important to relate the "unstructured" (in crystallographic terms) information on the concentration of individual chemical elements in the GS fractions to its real meaning, i.e. the "structural" information on the concentration of specific minerals.

2. Data Base

The samples were collected from moraines and very proximal glacio-fluvial deposits from (i) the Rhone, Damma and Tiefer glaciers draining the Central Aar massif in Central Alps of Switzerland, and (ii) the Vermunt, Jamtal, and Chalaus glaciers draining the Silvretta crystalline massif of the Eastern Alps in Austria.

The latter massif is largely composed of amphibolites, orthogneisses, and amphibolite-grade metapelites, which is reflected in the pebble populations of the moraines from the sampled glaciers. Pebbles are composed of 50 to 90% amphibolites and amphibole-rich gneisses, 10 to 50% garnet-rich gneisses, and 0 to 30% biotite-bearing quartzschists. In some places marble occur as well, however, this is subordinate. Thus, the most relevant detrital minerals to be expected are (in roughly decreasing order) feldspar, amphibole (mainly hornblende), quartz, garnet and sheet silicates (biotite, muscovite, and chlorite), as well as epidote-group minerals (Schweinehage 2000). Accessories may include apatite, Ti-bearing phases (rutile, titanite, and ilmenite) as well as clinopyroxene.

The glaciers draining the Central Aar massif erode almost pure granitoid lithologies (granites, granodiorites, orthogneisses, etc.) from the so-called central Aar granite. The granitoids are mainly composed of feldspar (61-65%), quartz (21-35%), and mafic minerals ranging from 1-14% (Debon and Lemmet 1999). Monzogranites and granodiorites of the Central Aar granite s.str. exhibit a somewhat narrower range, especially regarding quartz content (quartz 30-34%, feldspar 58-66%, mafics 4-8%). Characteristic mafic and accessory minerals are biotite, garnet, titanite, allanite (epidote group), and sometimes fluorite.

The sediment samples were separated in up to eleven grain-size fractions ranging from very coarse sand (1 – 2 mm, $-1 < \phi < 0$) to clay (< 2 μm, $\phi > 9$) by sieving of the sand fractions and centrifuge-aided settling of the finer fractions. Each sediment grain-size fraction was powdered, fused using lithium metaborate, and subsequently analysed by X-ray fluorescence. Ten major element oxides (SiO_2, Al_2O_3, TiO_2, total Fe as Fe_2O_3, MnO, MgO, CaO, Na_2O, K_2O, P_2O_5) and several trace elements (not considered here) were measured. Figure 1 shows a box-plot representation of the raw variables (major element oxides) for the analyzed data set, separated for the two different sources showing strongly contrasting compositions. Granitoids are higher in SiO_2 and K_2O, whereas amphibolites are higher in MgO, Fe_2O_3, CaO throughout all GS fractions. Other elements show more complex patterns such as converging concentrations towards finer grades (e.g. TiO_2, MnO) or changing predominance at different grain-size grades (e.g. Al_2O_3, P_2O_5 ; Fig. 1).

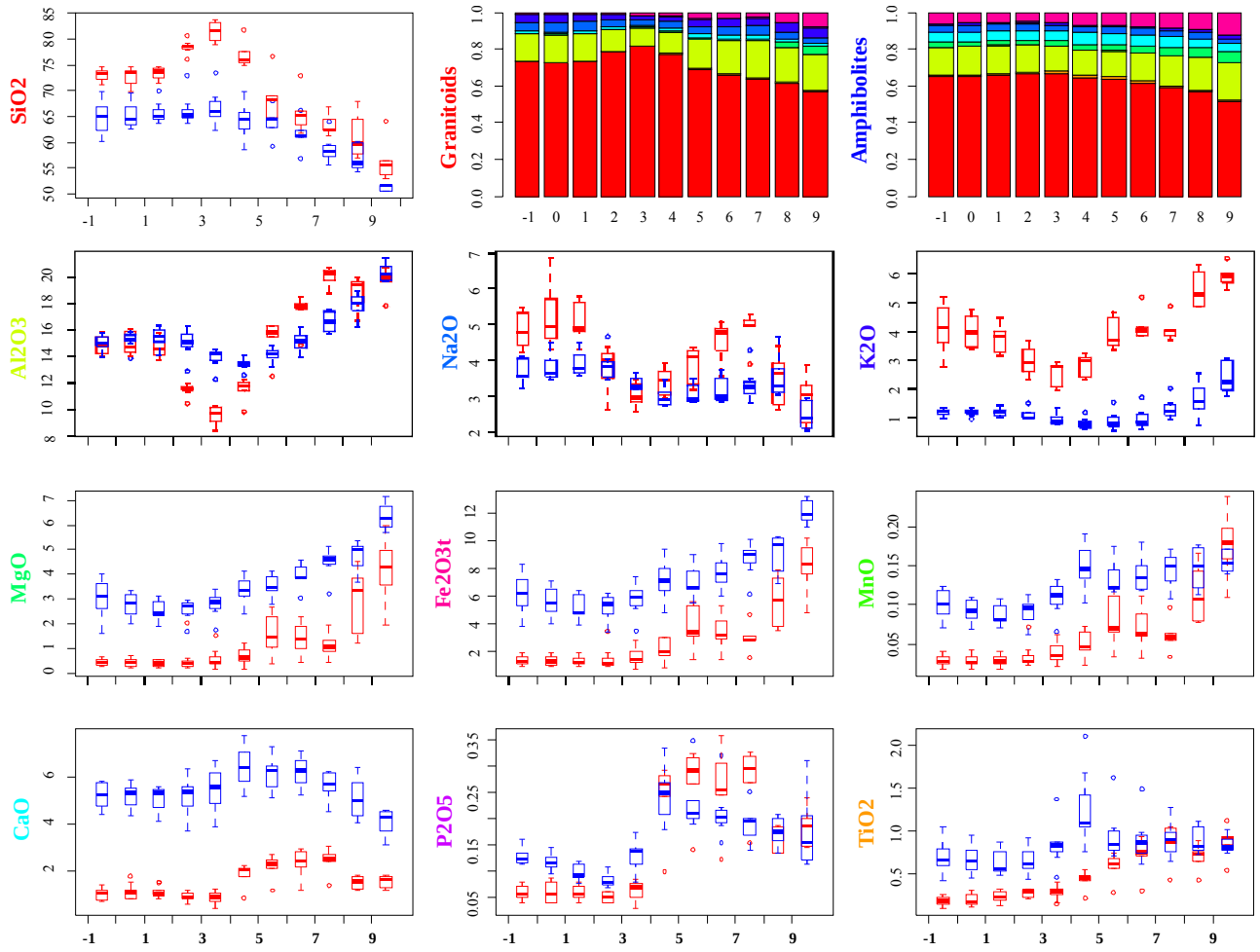

Figure 1: Box plots for the observed major element compositions (raw data in wt.-%) versus grain size fractions from very coarse sand ($-1 < \phi < 0$) to clay ($\phi > 9$) showing contrasts between granitoid samples from the Aar massif (red) and amphibolite-samples from the Silvretta massif (blue). Upper middle and right graphs show overall composition for the two sample groups. Note that the bar colours are used again with the component names.

3. Statistical Methods

Compositions are vectors of positive components that are usually "closed", i.e. the components sum up to a constant which is typically 1 (or 100%):

$$\mathbf{x} = (x_1, x_2, ..., x_D) \quad \text{with } x_i > 0 \text{ and } \Sigma\, x_i = c \ (i = 1, 2, \ldots, D).$$

The sample space for D-part compositional data is known to be the simplex S^D (Aitchison, 1986), not the D-dimensional real space $\mathbf{R}^D$. In this case, the golden rule is to work on log-ratios of parts (Aitchison, 1997), which typically involve the use of the centered log-ratio transformation (clr, Aitchison, 1986), some log-ratio coordinates or, as we will do here, the set of all $D(D\text{-}1)/2$ possible pairwise log-ratios.

A first glance at the structure of variability of the data set may be obtained through the compositional biplot, a well-known 2D representation of the singular value decomposition (SVD) of a centered clr-transformed data set. As pointed out by Aitchison (1997), in a compositional biplot links joining two variables represent the log-ratio of that pair of variables. Lengths of well-captured links are proportional to the pairwise log-ratio variance, whereas the cosine of the angle between two links corresponds to correlation coefficient between the corresponding pairs of log-ratios. Dots represent each observation, and their projection onto a given ray or link indicates how richer/poorer in the considered variable(s) that particular observation is, with respect to the average of the data set.

After looking at the biplots and clr-boxplots, it will become obvious that grain-size provides one of the strongest controls on compositional variability. It is thus reasonable to try a compositional linear model, which in our case will include a linear trend and one or two step functions, together with a possible source rock effect:

$$\mathbf{x}_g(\phi) = \mathbf{x}_g(0) \oplus \phi \odot \mathbf{a}_g \oplus I(\phi>4) \odot \mathbf{b}_4 \oplus I(\phi>4) \odot \mathbf{b}_8,$$
$$\mathbf{x}_a(\phi) = \mathbf{x}_a(0) \oplus \phi \odot \mathbf{a}_a \oplus I(\phi>4) \odot \mathbf{c}_4 ,$$

where $\mathbf{x}_g(0)$ and $\mathbf{x}_a(0)$ are the coarse sand ($0 \le \phi < 1$) compositions for granodioritic and amphibolitic source rocks, $\mathbf{a}_g$ and $\mathbf{a}_a$ are the respective slopes of the linear model, and $\mathbf{b}_i$ as $\mathbf{c}_i$ represent jumps at $\phi > i$ for each of the two source rocks. The function $I(\phi>i)$ is a unitary jump at $\phi > i$. We consider the following competing models:

[1] the same slope for both source rock, i.e. $\mathbf{a}_a = \mathbf{a}_g$ (named *full model* in the following)
[2] a different slope in each source rock (i.e., a model for amphibolites, comparable to the one fitted for granitoid source rocks by von Eynatten and Tolosana-Delgado, 2008)

Compositional linear models become classical linear models once we express all involved compositions in log-ratios (or in clr, or in coordinates). For instance, using the pairs of components i and j, we find

$$\log \frac{x_{g,i}(\varphi)}{x_{g,j}(\varphi)} = \log \frac{x_{g,i}(0)}{x_{g,j}(0)} + \log \frac{a_{g,i}}{a_{g,j}} \cdot \varphi + \log \frac{b_{4,i}}{b_{4,j}} \cdot I(\varphi > 4) + \log \frac{b_{8,i}}{b_{8,j}} \cdot I(\varphi > 8) \quad (1)$$

, and

$$\log \frac{x_{a,i}(\varphi)}{x_{a,j}(\varphi)} = \log \frac{x_{a,i}(0)}{x_{a,j}(0)} + \log \frac{a_{a,i}}{a_{a,j}} \cdot \varphi + \log \frac{c_{4,i}}{c_{4,j}} \cdot I(\varphi > 4) \quad (2)$$

.

A set of equations like the preceding ones will be fitted to all possible pairwise log-ratios. As our goal is to detect which parts are affected by the linear trend and which by the step functions, we will obtain standard univariate confidence intervals for the model coefficient, under the hypotheses [1] and [2]. Those ratios which slope is not significant may be taken as unchanged under grain size evolution, i.e. whichever process progressively comminutes or reduces grain size treats both components indiscriminately. Similar conclusions may be reached with respect to ratios with a non-significant jump coefficient: whichever process produces those discontinuities, it treats both components in the same way. This must be considered an exploratory approach, as a rigorous treating would imply multiple testing of null coefficients for several log-ratios simultaneously. This was explored by Tolosana-Delgado and von Eynatten (2010) by suggesting a method to automatically find a basis where one easily tests the desired hypotheses of subcompositional independence for each explanatory variable. However, this approach was discarded in this case, because the current implementation is extremely memory-demanding.

As the available explanations for these trends and jumps will be mostly related to mineralogy, the final steps of the analysis will be the geometric reconstruction of a possible mineralogical composition of each sample, compatible with the observed geochemistry. This is done following Tolosana-Delgado et al (in press) geometric algorithm, briefly summarized here and in Tolosana-Delgado (2011). Assume that one knows which mineral phases are present, as well as their stoichiometric composition. Each mineral may be written as a composition of S^D, and within a row of a matrix $\mathbf{T}$ (called the stoichiometry matrix). If we had available $\mathbf{z}$ the mineral composition of our sediments, then each of our geochemical compositions would satisfy $\mathbf{x}=\mathbf{z}\cdot\mathbf{T}$. But as $\mathbf{T}$ is not square and not invertible, we have to use Moore-Penrose generalized inversion. Take the SVD of $\mathbf{T}=\mathbf{U}\cdot\mathbf{D}\cdot\mathbf{V}^t$, and note that the columns of $\mathbf{U}$ identify a basis of the mineral simplex S^P. As the $P>D$, there are some null singular values in the matrix $\mathbf{D}$. Denote by $\mathbf{D}_r$ the diagonal matrix of non-zero singular values, the matrix of columns of $\mathbf{U}$ linked to a non-zero singular value as $\mathbf{U}_r$, and the matrix of remaining columns as $\mathbf{W}$. Then the set of all solutions is

$$\mathbf{z}(\boldsymbol{\lambda}) = \mathbf{x}\cdot\mathbf{V}\cdot\mathbf{D}_r^{-1}\cdot\mathbf{U}_r^t + \boldsymbol{\lambda}\cdot\mathbf{W}^t \qquad (3)$$

where $\boldsymbol{\lambda}$ is a real vector with $P–D$ components. The columns of $\mathbf{W}$ represent thus mineral exchanges which do not modify the overall geochemistry of the mixture. Not all solutions $\mathbf{z}(\boldsymbol{\lambda})$ are valid compositions, as some $z_i(\boldsymbol{\lambda})<0$. If it exists, the set of valid solutions with all non-negative components, is a convex hull resulting of intersecting the hyperplane of Eq. (3) with S^P. We take as representative solution the center of this convex hull (in the geometry of $\mathbf{R}^P$).

4. Results

4.1 Descriptive Analysis

Biplot analysis reveals striking, unexpected similarities with respect to the covariance structure of the two data sets. MgO, P_2O_5, and Na_2O are most relevant for the overall variability, with K_2O being additionally important for the amphibolite data set (Fig. 2). Major elements like Si, Al, K and Na (in the following called "felsic" elements) that are typical for minerals enriched in felsic rocks such as alkali feldspar, muscovite and quartz, plot together on one side of the biplot (positive loading on PC-1). In contrast, elements typically associated with minerals enriched in mafic rocks (Mg, Fe, Mn; in the following called "mafic" elements, abundant in most sheet silicates, garnets, epidotes and amphiboles) plot to the other side (negative loading on PC-1). A third pole is clearly visible in the granitoid dataset, defined by strong positive loading (PC-2) of P_2O_5 that appears to be related to CaO, and most likely reflect the mineral apatite. This relation is still visible in the amphibolite biplot, however, the three-pole structure of granitoids is less clear in amphibolites, as P_2O_5 appear to be more associated with the mafic elements. High loading of CaO on PC-2 and opposed strong negative loading of K_2O on PC-2 (amphibolites) may either reflect contrasting feldspar types (i.e. Ca-rich plagioclase vs. K-rich K-feldspar) or, more likely, plagioclase (and some apatite) enrichment in some coarse to medium grain-size fractions relative to an enrichment of K-rich sheet silicates (muscovite/biotite) in fine fractions. PC-2 is mostly complementary in granitoids

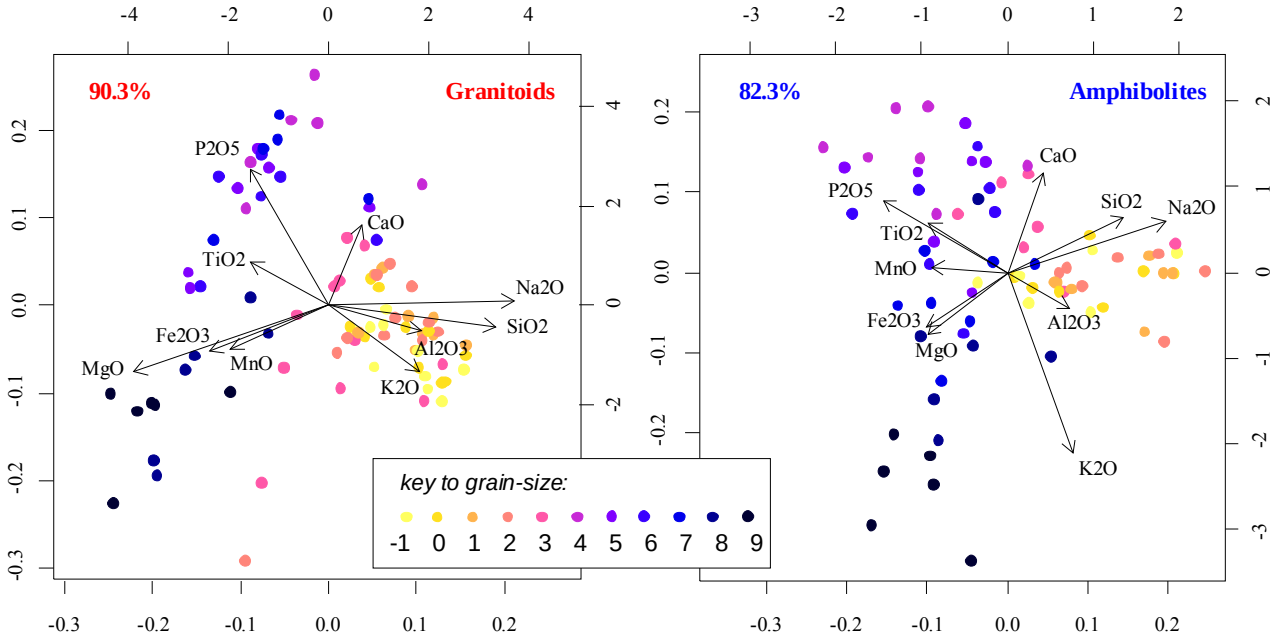

Figure 2: Compositional biplots for both data sets using first (x-axis) and second principal component (y-axis), with colour coding for grain-size range. Percentage indicates proportion of total variability captured by PC-1 (71.2% inn granitoids, 47.7% in amphibolites) and PC-2 (19.0% and 34.5% respectively). Grain size category i includes all grains with sizes $i \leq \phi < i+1$; $\phi=9$ includes all particles with $\phi>9$. Recall that rays represent clr-transformed variables and should not be interpreted.

(representing just a 19% of the variance, in contrast with the ~70% captured by PC-1), whereas in the case of amphibolites its contribution to the variance (~35%) is comparable to that of PC-1 (~47%).

Individual grain size fractions from different samples plot close to each other revealing strong grain-size control on sediment composition (Fig. 2). Sand-sized fractions ($-1 < \phi < \sim 3$) cluster on the felsic elements Si, Al, and Na (including K for granitoids) against low mafics, whereas fine-grained silt and clay fractions ($\phi > 7$-8) are clearly associated with high proportions of mafic elements Mg, Fe, and Mn (including a K-enrichment trend for amphibolites) in contrast to low Na and Si. Intermediate grain size fractions ranging from very fine sand or very coarse silt ($3 < \phi < 5$) to medium silt ($\phi = 6$-7) cluster at high proportions of P_2O_5, CaO, and TiO_2 vs. low K (may include also some high MnO for the amphibolite samples). This observation strongly suggests that specific minerals are enriched in certain grain-size fractions. Specifically, quartz and feldspar are expected to be enriched in sand fractions, while biotite and chlorite (and maybe amphibole) appear to be enriched in the finest fractions. Apart of constituting a mixture of these two "endmembers", the intermediate fractions appear to be enriched in accessory heavy minerals such as apatite (and some other phosphate minerals?), titanite and/or rutile, and probably garnet.

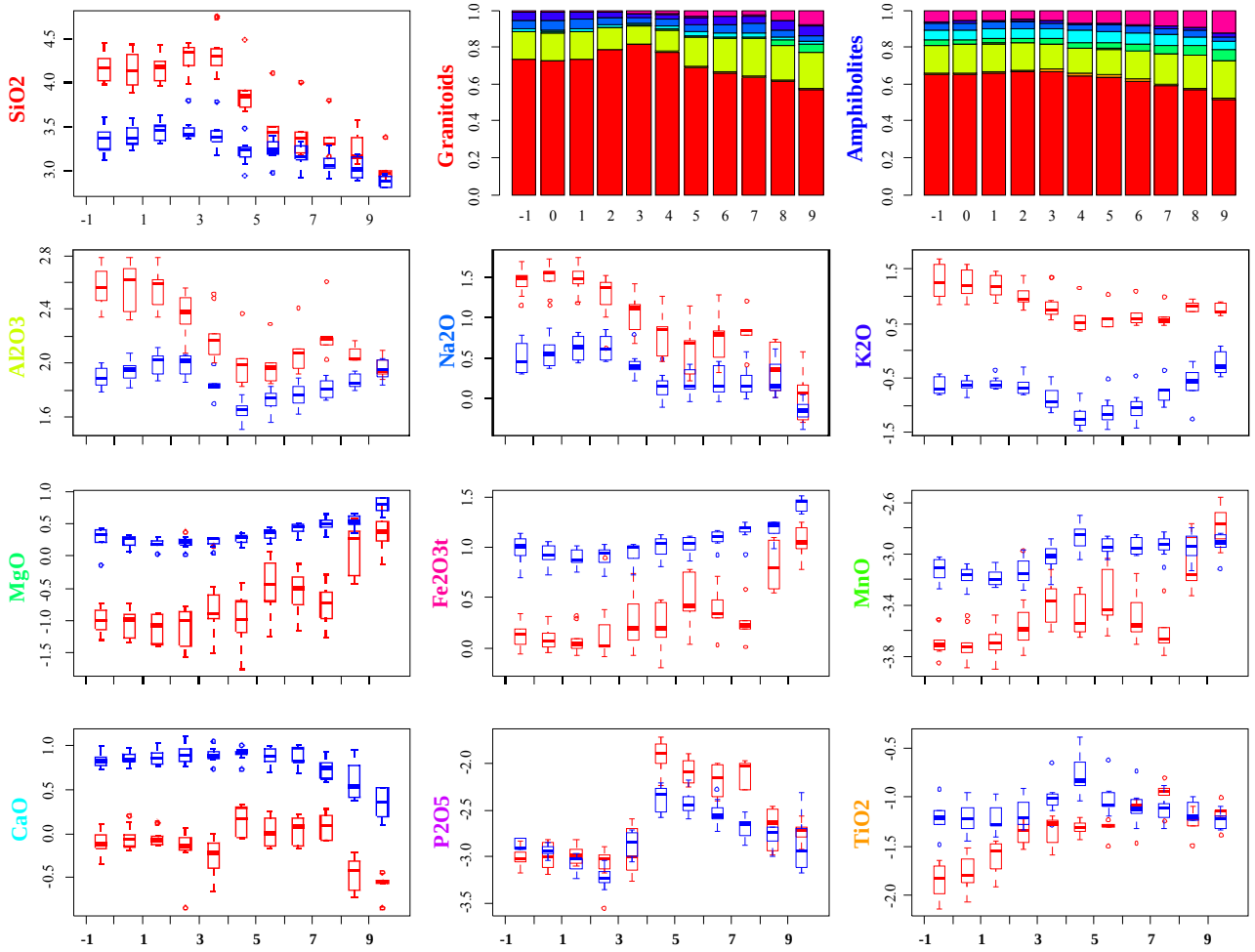

Figure 3: Box plots of the clr-transformed major element compositions for granitoid (red) and amphibolite-samples (blue). Upper middle and right graphs show overall composition for the two sample groups. Note that the bar colours are used again with the component names.

Box-plots of individual elements, represented in clr-scale (Fig. 3), corroborate several of these details, especially (i) the overall increase of Mg and Fe with decreasing grain size (as well as K especially in amphibolite); (ii) an overall decrease of Si, Al, and Na with decreasing grain size; and

(iii) a specific break within this overall trends at around $\phi = 4$ that is most clearly reflected by P_2O_5 in both data sets, as well as by Ca for granitoid samples and by Ti and Mn for amphibolite samples. Other elements such as Si, Na, and K show at least strong gradients between $\phi = 3$ and $\phi = 5$. The granitoid data set also shows a break at around $\phi = 8$ for several elements (Ca, Mg, Fe, P, Mn; see also von Eynatten and Tolosana-Delgado, 2008). This combination of an overall trend with distinct breaks in clr-scale suggest approximation of the GS to geochemistry relation by a log-linear model including a step function at $\phi = 4$ (see sections 3 and 4.2).

Beyond grain-size relations, the boxplots reveal the differences between the two source areas across GS grades. Interestingly, most elements in both subsets converge towards finer grades, both in raw data concentration (Fig. 1) and clr-scale (Fig. 3), leading to significant overlap between sediments from amphibolites and granitoids at the finest grades. Some elements (Ca, K, and with less confidence Fe and Mg), however, do not overlap at the finest grades (Fig. 3), implying that Ca and K are most suited to discriminate between the two major sources even at the finest grain-size fraction like fine silt or clay (Fig. 4, see Ca vs. K panel).

4.2 Regression Analysis: major element composition vs. grain size

This strong control of grain size on geochemical composition has been modelled with a compositional linear trend (Eqs. 1-2). Figure 4 compares the linear model obtained by von Eynatten and Tolosana-Delgado (2008) for the granitoid data set with the equivalent model of Eq. (2) hypothesis [2] for amphibolites; as well as a joint model (Eqs. 1 and 2) under hypothesis [1]. This figure only includes those pairwise log-ratios showing the most interesting concordant or discordant

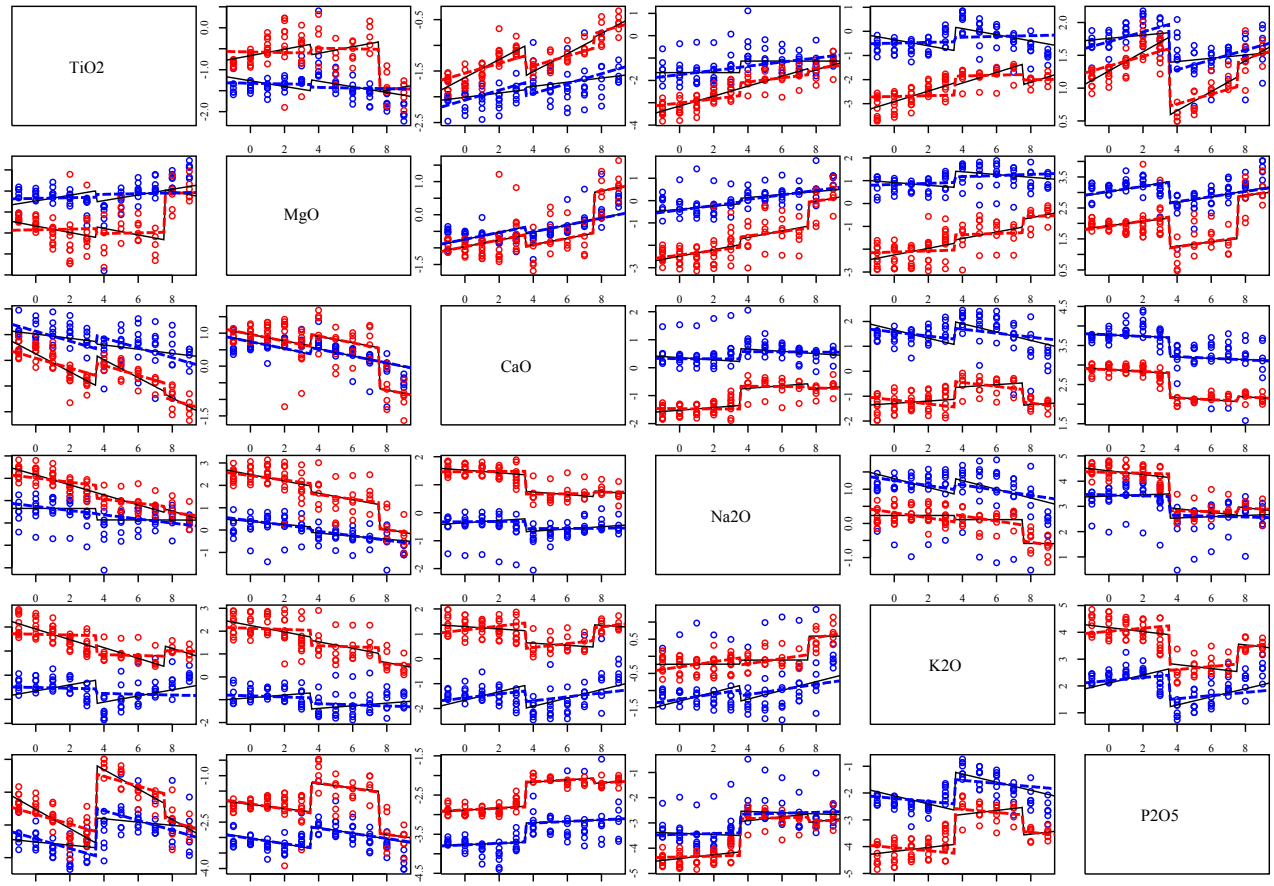

Figure 4: Selected pairwise log-ratios to compare the full model (coloured dashed lines; blue – amphibolite, red – granitoids) with the granitoid (von Eynatten and Tolosana-Delgado, 2008) and amphibolite particular models (black thin lines). Each diagram shows the log-ratio of two components (row/column) against GS. One outlier sample (RT2-11, blue, rich in marble detritus – see for instance Ca ratios) was not included in the computations.

patterns. Other elements behave mostly like the represented ones: MnO and $Fe_2O_3^t$ closely follow MgO; Al_2O_3 and especially SiO_2 behave similar to Na_2O.

With the notable exception of those involving TiO_2 and less strongly K_2O, all three models strikingly coincide in most pairwise log-ratios. In fact, the visual fit for those ratios involving these two parts is relatively bad: they would rather require in the amphibolites a three-segment continuous model with a different trend in the interval $3<\phi<5$. As was pointed by von Eynatten and Tolosana-Delgado (2008), the general trend is an enrichment in mafic elements at the expense of felsic elements, whereas the segment $4<\phi<8$ is characterized by Ca-P enrichment relative to all other parts. In amphibolites, the linear trend is mostly the same, though no jump is visible at $\phi=8$, and the jump at $\phi=4$ rather occurs smoothly between 3 and 5 in the elements P-Ti-Ca.

However, many of these slopes and jumps are rather small. Figure 5 visually displays their significance, comparing the results under hypothesis [1] and hypothesis [2] (see chapter 3). Simply counting which elements are involved in significant coefficients for both hypotheses, the picture is pretty clear for the step at $\phi=4$, being dominated by P and K: among 14 "double-significant" pairs, 7 include K and 6 include P, contrasted with Al, Ca, Fe, Mg, Ti and Mn (the ratios Al/Ca, Al/Fe and Na/Ca are also significant). This implies an increase in Ca and P, mostly at the expense of K. This occurs quite abruptly at $\phi=4$ in the granitoids, and is rather smoothened in the amphibolites. The explanation given in von Eynatten and Tolosana-Delgado (2008) was that this effect is inherited from the typical grain-size of apatite in the granitoid host rocks.

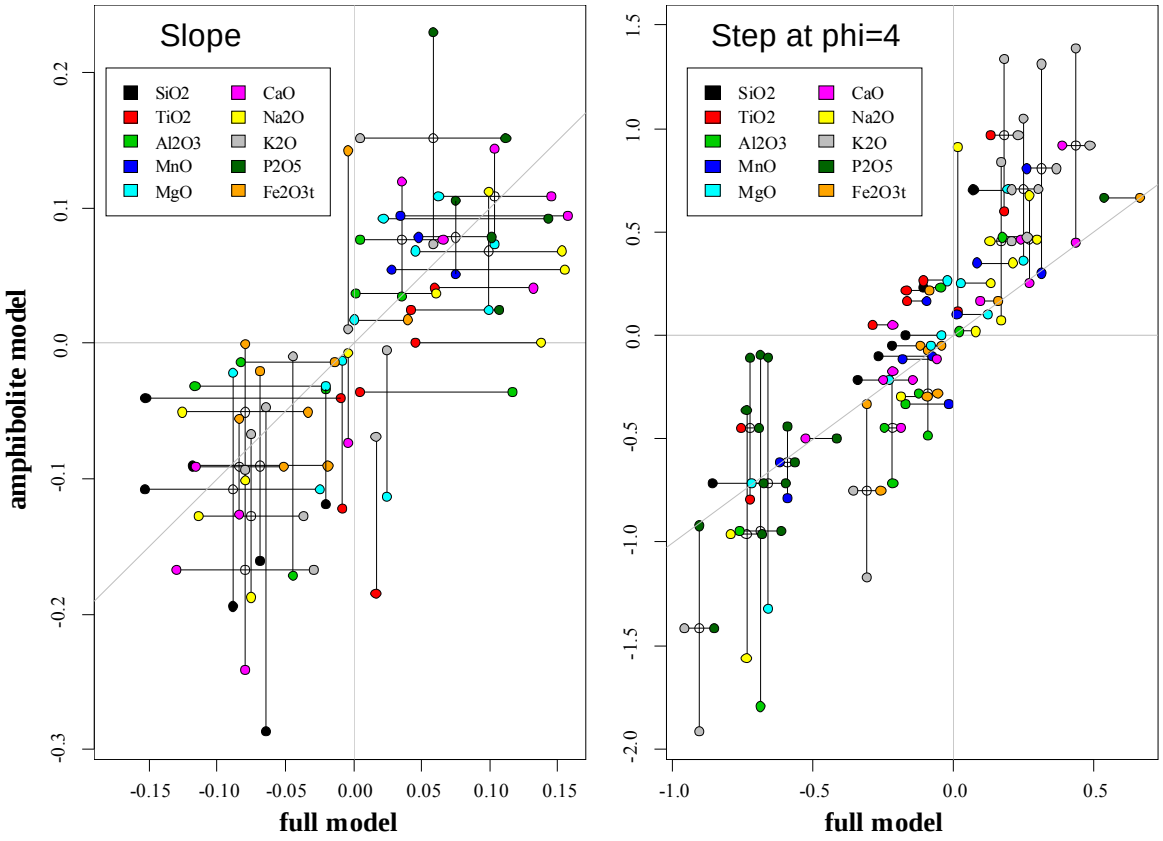

Figure 5: Crossplots showing *significant* coefficient estimates and estimation confidence intervals (95%) obtained for the global regression model (abscisas, horizontal segments) vs. the amphibolite model (ordinates, vertical segments), for the slope (left side) and the step at $\phi=4$ (right side). When the ratio is significant for both models, the crossing point of both segments shows an open circle. Colour indicates the two parts involved in the respective ratio (numerator in the lower/left limit and denominator in the upper/right limit of the segments).

The structure is less clear for the slope: among 11 "double-significant" pairs Ca is most frequently involved (4 times) followed by Na, Fe, Mg and K (each appearing three times). The

trend is mostly enrichment in Fe and Mg in contrast to Na and Ca, which is also nicely illustrated in the MgO-CaO and MgO-Na_2O log-ratios in Figure 4. These observations are almost identical for both suites (except for K that behaves either way) and, thus, the explanation given for granites, a progressive enrichment in sheet silicates and mafic minerals, is also valid for the amphibolite data set.

The trend exhibited for TiO_2 is different: while we observed homogeneous enrichment in case of granitoids source rocks (suggesting that this element is mostly involved in the same mineral phases than other mafics; von Eynatten and Tolosana-Delgado, 2008; Fig. 4), the amphibolites show a clear maximum in Ti log-ratios around ϕ=4 (see, e.g. TiO_2-K_2O in Fig. 4). This suggests that most Ti may rather be hosted in a resistant mineral, with a characteristic size around ϕ=4, which is difficult to comminute. This is also suggested by the biplots (Fig. 2), where TiO_2 ray occupies an intermediate position between P_2O_5 (and medium sized grains) and the mafics (and fine materials) in granitoids, but is clearly associated with P_2O_5 (and intermediate grain sizes) in amphibolites. At the same time, note that the ratio of variances of PC-2 to PC-1 was much larger in granitoids than in amphibolites implying that a one-dimensional st raight compositional trend is more likely for the first data set (PC1 explains ~71% of total variability) than for the second, the amphibolite data set (~48%).

4.3 A plausible mineral reconstruction

As the relations between geochemical and mineral composition as well as mineral stability play such an important role in the interpretation we have done so far, it is necessary to obtain an estimate of this mineralogical composition. Using the stoichiometry listed in Table 1, we have obtained central mineral compositions as displayed in Figure 6. This shows clear trends of enrichment in sheet silicates (muscovite, biotite and chlorite groups) towards the fine-grained fractions, mostly at the expense of quartz (beginning from around ϕ= 3 to 4) and amphiboles (beginning from ϕ=6 to 7).

mineral	symbol	SiO_2	Al_2O_3	$Fe_2O_3^t$	MgO	MnO	CaO	Na_2O	K_2O	P_2O_5
quartz	qz	1	0	0	0	0	0	0	0	0
alkali feldspar	kfs	3	0.5	0	0	0	0	0	0.5	0
albite	alb	3	0.5	0	0	0	0	0.5	0	0
anortite	ano	2	1	0	0	0	1	0	0	0
muscovite	mus	3	1.5	0	0	0	0	0	0.5	0
biotite	bio	3	0.5	1.5	0	0	0	0	0.5	0
phlogopite	phl	3	0.5	0	3	0	0	0	0.5	0
apatite	apa	0	0	0	0	0	5	0	0	1.5
epiode	epi	3	1	0.5	0	0	1	0	0	0
clinozoisite	clz	3	1.5	0	0	0	2	0	0	0
almandine	alm	3	1	3	0	0	0	0	0	0
pyrope	prp	3	1	0	6	0	0	0	0	0
spessartine	sps	3	1	0	0	6	0	0	0	0
Fe-chlorite	fcl	5.67	2.67	4.5	0	0	0	0	0	0
Mg-chlorite	mcl	5.67	2.67	0	9	0	0	0	0	0
tremolite-actinolite	tract	8	0	1.25	2.5	0	2	0	0	0
pargasite	prg	6	1.5	1	2	0	2	0.5	0	0
tschermakite	tsch	8	2	0.75	1.5	0	2	0	0	0

Table 1: Stoichiometry of the mineral phases considered

These two mineral groups show their largest abundance in fine sand to medium silt fractions, just like apatite (not visible here). It is interesting to see that feldspar abundances are rather constant in all grain sizes, and where they decrease, it is because either quartz or amphiboles have a maximum. The sum of all felsic minerals (quartz, feldspar) mostly show a constant or slightly increasing trend up to ϕ=2-3, and from that point on it clearly decreases towards finer fractions.

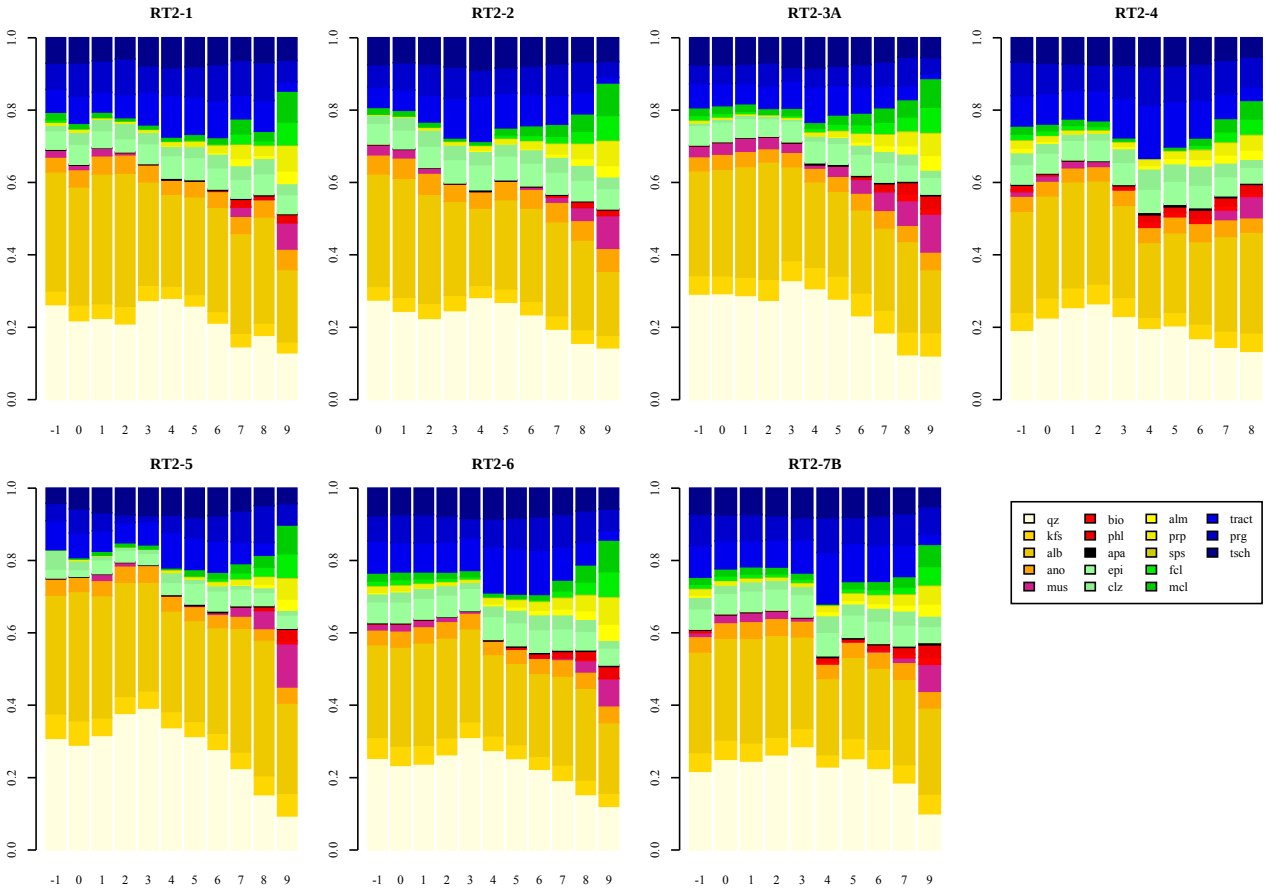

Figure 6: Barplots showing a plausible mineralogical composition for each sediment sample and grain size. Similar colours show minerals of the same family: feldspars (orange), biotite-phlogopite group (red), epidote group (pale green), garnets (yellow), chlorite (green) and amphibole (blue). Quartz (whitish), muscovite (pink) and apatite (black) do not belong to any of these groups. For mineral abbreviations see Table 1.

Discussion and Conclusions

The observed general trend show striking similarities for the full model based on the entire data set as well as the amphibolite model. The trend reflects progressive enrichment of sheet silicates (biotite-phlogopite, chlorite, and muscovite) with decreasing grain size, at the expense of quartz, and – to a lesser degree – feldspar. This is exemplarily illustrated in the MgO-Na_2O log-ratio (see Fig. 4; MgO may be substituted by Fe_2O_3 or MnO, Na_2O may be substituted by SiO_2 or Al_2O_3), and strongly underlines previous results based solely on granitoids source rocks suggesting that comminution (working most efficiently on sheet silicates) in the dominating process generating this kind of sediment (von Eynatten and Tolosana-Delgado 2008). The abundant occurrence of amphibole minerals in the new amphibolite data set (Fig. 6) does not significantly change this general picture.

The step function at ϕ=4 appears to be independent of the source rock, however, partly different elements are responsible for the step in the amphibolite and the granitoid model. For granitoids, the step is mostly caused by strong relative enrichment of apatite in the very fine sand to coarse silt

fraction. This holds also for the amphibolites, as indicated by the high number of log-ratios involving P in the numerator that are significant for a positive step at ϕ=4 in both the full and the amphibolite model (Fig. 5). SiO_2 is not involved significantly in the step for the amphibolite model however, most log-ratios involving SiO_2 in the numerator are peaking at ϕ=3-4 in both data sets, and steeply decrease thereafter implying that this is an effect of inherited (minimum) crystal sizes of quartz. Mineral calculations with quartz peak at ϕ=2-4 (Fig. 6) and support this interpretation, i.e. beyond fine to very fine sand quartz crystals are difficult to further comminute in the given settings. Amphiboles are peaking at slightly finer grades (ϕ=3-5) and decrease much slower towards finer GS (see below). For the amphibolites the step at ϕ=4 seems to be less precisely defined and more likely reflects a transitional interval from ϕ=3 to ϕ=5. With respect to chemistry, this is clearly visible on Ti (in contrast to, e.g., Si, Al, Na, Mg, Fe, K). Therefore, Ti is most likely hosted in amphiboles (explaining quite similar behaviour although Ti is not involved into the mineral calculations; Table 1), and/or in some accessory phases resistant to comminution (e.g. titanite, rutile, ilmenite) for the amphibolites, while it is mostly hosted in sheet silicates (biotite) for the granitoid data set.

The step function at ϕ=8 observed for the granitoids model is missing in the amphibolite model and, consequently, in the full model. This may be due to continuous fragmentation of amphibole (perfect cleavage) having a high content peaking at around ϕ=3-5 (Fig. 6) that slowly decreases towards finer grades, and that may smooth the trend towards finer grades. Also, apatite may not have such a characteristic lower size limit at ϕ=7-8.

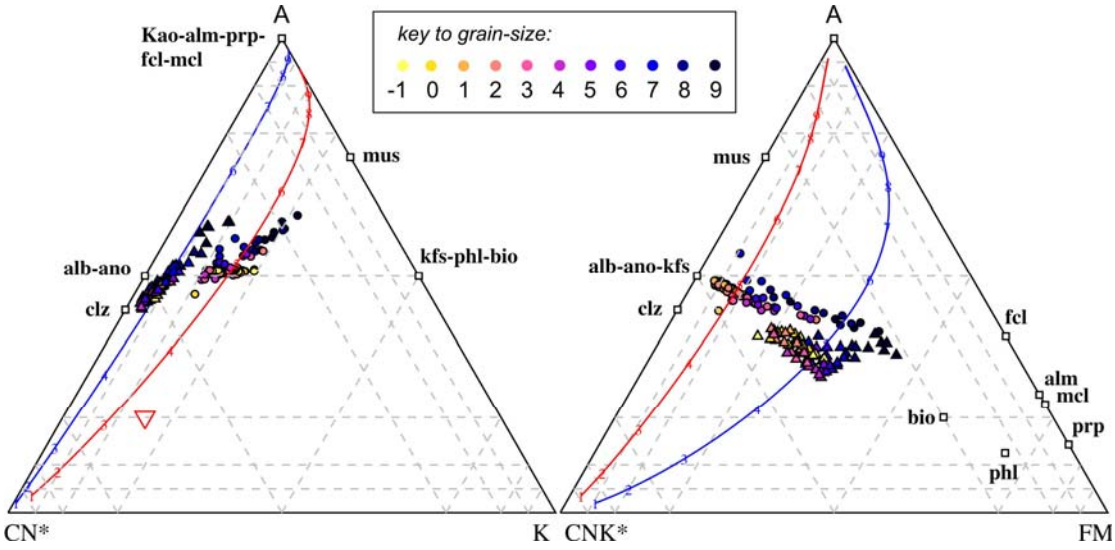

Figure 7: A-CN-K and A-CNK-FM diagrams according to Nesbitt and Young (1984): A= Al_2O_3, C= CaO, N= Na_2O, K= K_2O, F= Fe_2O_3, M= MgO; all in molar proportions. Red and blue lines indicate chemical weathering trend according to von Eynatten et al. (2003) adjusted to coarse sand composition for average amphibolite and granitoid samples, respectively. For Mineral abbreviations see Table 1.

Chemical weathering is most frequently displayed and quantified in A-CN-K and A-CNK-FM diagrams according to Nesbitt and Young (1984), which describe the principal enrichment of Al at the expense of Ca, Na, and K. Based on this principle we can clearly preclude chemical weathering as a significant process because the observed trend and the pairwise logratios are essentially unrelated to both systematic Ca, Na, and/or K depletion or Al enrichment (Fig. 4). Moreover, geometric mineral endmember modelling has shown that there is no noticeable progressive decrease of feldspar with respect to quartz. Slightly increasing values for the Chemical Index of Alteration (Nesbitt and Young, 1984) with decreasing grain size are related to the enrichment of sheet silicates in the finer fractions (Fig. 7).

To summarize, we observe a clearly dominating and similar process for both data sets, although the geological settings strongly contrast with respect to mineralogy and geochemistry of the source rocks. This process is comminution due to glacial forces in combination with negligible chemical alteration. Source rocks are relevant for the distribution of individual elements among specific minerals and the inherited grain size and resistibility of these minerals to mechanical forces, leading to differences in relevance and interpretation of certain steps in the relation of grain size vs. composition.

References

Aitchison, J. (1986) *The Statistical Analysis of Compositional Data*. Chapman & Hall Ltd., London, reprinted in 2003 with additional material by The Blackburn Press.416 p.

Aitchison, J. (1990). Relative variation diagrams for describing patterns of compositional variability. Mathematical Geology, 22, 487-511.

Aitchison, J. (1997). The one-hour course in compositional data analysis or compositional data analysis is simple. In: V. Pawlowsky-Glahn (Ed.), *Proceedings of IAMG'97 – The third annual conference of the International Association for Mathematical Geology*, pp. 3–35. International Center for Numerical Methods in Engineering (CIMNE), Barcelona, 1100 p.

Debon, F. and Lemmet, M. (1999). Evolution of Mg/Fe ratios in the Late Variscan plutonic rocks from the External Crystalline Massifs of the Alps (France, Italy, Switzerland). Journal of Petrology, 40: 1151–1185

Nesbitt, H. and G. Young (1984). Prediction of some weathering trends of plutonic and volcanic rocks based on thermodynamic and kinetic considerations. Geochim. Cosmochim. Acta, 41: 1523–1534.

Schweinehage, R. (2000): Metamorphite der Silvrettadecke / Ostalpen: Thermobarometrische und geochemische Untersuchungen zur präalpidischen Entwicklung. Dissertation, Universtät Tübingen, 330 pp.

Tolosana-Delgado, R., von Eynatten, H. (2010). Simplifying compositional multiple regression: Application to grain size controls on sediment geochemistry. Computers and Geosciences, 36, 577-589.

Tolosana-Delgado, R., von Eynatten, H., Karius, V. (in press). Constructing modal mineralogy from geochemical composition: a geometric-Bayesian approach. Computers & Geosciences (2010-online, doi:10.1016/j.cageo.2010.08.005.

Tolosana-Delgado (2011). Unmixing compositional data with Bayesian techniques. In: Proceedings of CoDaWork'11 (this volume)

von Eynatten, H., Barceló-Vidal, C., Pawlowsky-Glahn, V. (2003). Modelling compositional change: the example of chemical weathering of granitoid rocks. Mathematical Geology, 35: 231–251.

von Eynatten, H., Tolosana-Delgado, R. (2008). A log-linear model of grain size influence on the geochemistry of sediments. In: J. Daunis i Estadella & J.A. Martin-Fernandez (eds.) Proceedings CoDaWork'08 – 3nd Compositional Data Analysis Workshop, S3-1, 18 p., Girona.

Weltje, G.J., von Eynatten, H. (2004). Quantitative provenance analysis of sediments: review and outlook. Sedimentary Geology, 171: 1–11